



# Generation and Transport of Smoke Components

*Kathryn M. Butler and George W. Mulholland, National Institute of Standards and Technology, 100 Bureau Drive, Gaithersburg, MD 20899-8665, USA*

**Abstract.** Smoke is a mixture of gases, vapors, and suspended particulate matter, or aerosols. The nature of the aerosol component of smoke can play a significant role in its deposition in the fire environment and in its lethal and sublethal effects on people. This paper presents the current state of knowledge about smoke aerosol phenomena that affects smoke toxicity: soot generation, fractal structure of soot, agglomerate transport via thermophoresis, sedimentation, and diffusion, agglomerate growth through coagulation and condensation, and the potential for the aerosols to transport adsorbed or absorbed toxic gases or vapors into the lungs. Tables are included for measured smoke yields and aerodynamic particle sizes, equations and references are provided for the smoke agglomerate transport properties and wall loss, and key literature references are provided for adsorption of irritant gases on soot particles and water droplets and the toxicity of nanosize particles.

**Key words:** smoke aerosol, smoke generation, smoke transport, smoke toxicity, ultrafine particulates

## Introduction

There is increasing concern about sublethal effects of smoke generated by fires. The eye and lung irritation due to irritant gases and aerosols and the confusion due to asphyxiants may slow escape or cause incapacitation. The inhalation of a large concentration of soot and toxic gases may lead to lung edema and inflammation, causing death a short time after the fire. This paper focuses on the information needed to assess the smoke aerosol exposure of an individual in a fire. The key smoke property information is the particle yield, the particle size distribution, and the type and amount of toxic gases adsorbed on the particulate. Factors affecting smoke transport include the fire size and building geometry, the change in size distribution resulting from coagulation and condensation, and particle losses due to thermophoresis, sedimentation, and diffusion. This information would enable an estimate of the smoke exposure of an individual at a target location in a building.

A second possible application of this paper concerns the major cleanup challenge posed by smoke deposition during and after a fire. Knowledge of the smoke yield, smoke size distribution, and transport and deposition processes are necessary for developing a model of smoke deposition resulting from a fire. Protection of critical equipment could be improved by using such a model to modify building design.

Smoke is a mixture of gases, vapors, and particulates. The latter include both microdroplets formed from condensed organic vapors and carbonaceous agglomerated structures (soot) consisting of hundreds up to many thousands of nearly spherical primary particles. A

range of adverse health effects is associated with inhalation of smoke aerosols, depending on the amount and location of their deposition within the respiratory tract. The depth of penetration into the lungs and the likelihood of being exhaled depend on the particle size. The degree of damage depends on the quantity of deposited particles, which is related in turn to the concentration of smoke aerosol in the inhaled air, on their shape, and on their toxicity. The damage can cause immediate effects such as a coughing response or long-term effects such as the suspected role of smoke inhalation in the development of cancer. In this paper the focus is on the short-term effects that impair the individual's ability to escape from the fire and to survive its immediate aftermath.

We focus on flame-generated smoke. Many of the exposures of concern are remote from the fire source, which requires a strongly buoyant plume generated by a flame. Although non-flaming sources produce high yields of toxic products that may spread beyond the room of origin under certain circumstances [1], this will not be addressed in this paper. This document contains three sections: (1) Smoke aerosol characteristics, including smoke yield and size distribution; (2) Smoke transport, changes, and losses; and (3) Adsorption of toxic gases on smoke particulates.

### **Physical and Chemical Characteristics of Smoke Aerosol**

An assessment of conditions within the lungs must begin with information about the initial character of particulate matter as it emerges from the fire. Soot formation and growth involves a number of processes. First, the fuel pyrolyzes from the surface as fuel fragments. In the high temperature flame environment, these fragments react to form acetylene, benzene, and radical species including H, OH, and small hydrocarbon radicals. The one-ring benzene undergoes a number of reactions involving acetylene and the radical species leading to multiple-ring species termed polycyclic aromatic hydrocarbons (PAHs). The PAHs continue to grow to ultimately form the smallest soot particles, which are on the order of a few nanometers [2]. Subsequent particle growth takes place by surface addition of acetylene and particle-particle collisions, termed coagulation, followed by coalescence into a single particle. The early soot loses hydrogen forming a solid particle that no longer coalesces. The size of the particle at this step is on the order of 0.02  $\mu\text{m}$  to 0.05  $\mu\text{m}$ . Subsequent growth occurs by agglomeration of these primary particles. This agglomeration process takes place in the flame, where some of the primary particles are partially fused, as well as in the post-flame region, where the agglomerates are held together by dispersion forces. As the smoke leaving the flame cools, vapor phase PAHs condense on the surface of the soot particle. The amount of condensed organics is generally less than 20% for overventilated fires; however, for underventilated fires the fraction can increase to 50% and the agglomerates develop a more agglutinated structure [3]. Smaller molecules, including water, benzene, other hydrocarbons, and acid gases, may adsorb on its surface. The surface area of a smoke particle and the chemical functionalities on that surface are of critical importance to the particle's subsequent growth and migration and to its ability to adsorb water and toxic gases. The topic of surface adsorption will be discussed later in this paper.

The focus of this section is on the smoke yield for flaming combustion and the size distribution of the agglomerates. These are key properties needed for modeling the impact of a fire on the inhalation conditions at a location some distance from the fire.

### **Smoke Yield**

Smoke yield, sometimes also referred to as the emission factor, is defined as the mass of smoke generated per mass of fuel burned. Values range from fractions of a percent to about 20% of the fuel mass. Fuels such as methane and wood undergoing flaming combustion populate the low end of this scale, and the high end typically represents fuels with an aromatic chemical structure.

The two major methods for determining smoke yield are the flux method and the carbon balance method [4]. The flux method consists of measuring the mass of smoke collected on a filter, the mass loss of the sample, and the ratio of the mass flow of air through the exhaust duct to the mass flow rate through the filter sample. The carbon balance method involves the determination of the carbon mass in the smoke aerosol as a fraction of the carbon mass in the total combustion products ( $\text{CO}_2$ ,  $\text{CO}$ , and smoke aerosols). These represent the major carbon-containing products of combustion for overventilated burning. By this method, the smoke yield is obtained as the product of the carbon fraction times the mass fraction of carbon in the fuel. In some studies [5], the mass concentration of the smoke is determined by a mass monitoring device such as a tapered element microbalance or by performing a light extinction measurement that is calibrated by a series of gravimetric measurements.

Smoke yield measurements are a challenge because of thermophoretic losses of the hot smoke to cooler sampling lines, the difficulty in accurately weighing filter samples, and the possible nonuniformity of the smoke concentration in the exhaust lines. The use of repeatability studies or of two independent measurements to check smoke yield measurements has been lacking. These factors may be responsible for some of the variability observed in the literature for smoke yield results for nominally identical fuels. Other factors affecting comparisons are incomplete specification of the burning material or the combustion mode (one sample may be collected only during flaming combustion while the other is collecting throughout the burning of the object including the smoldering phase), different sample sizes, different radiant fluxes to the sample, and different sample configurations.

Extensive small scale studies of fire product generation as a function of fuel type have been carried out by A. Tewarson using the ASTM E2058 fire propagation apparatus designed by the Factory Mutual Research Corporation [5]. In this experimental setup, small samples on the order of 100 mm wide by 600 mm high are ignited under a collection hood. Smoke generation rate is measured in the sampling duct above the hood using a light extinction measurement based on measuring the ratio of the incident to transmitted light intensity and a commercial smoke mass monitoring instrument. Table 1 lists smoke yields determined by Tewarson for a range of fuels under well-ventilated flaming conditions.

Table 1 illustrates that the amount of smoke generated is strongly dependent on the type of material being burned. Oxygen-containing fuels such as alcohols approach the smallest smoke yields, aromatics have the largest, and alkanes and alkenes are intermediate. Table 1 provides useful data for a wide range of simple fuels as well as for typical polymers found in buildings.

In general, smoke yield increases moderately with increasing fuel size. For a pool fire, Evans et al. [6] found that increasing the diameter from 0.085 m to 2 m increased smoke production from 0.06 g to 0.13 g of smoke per gram of crude oil. A comparison of large scale test results for sugar pine and rigid PU crib structures with those for cone calorimeter

**TABLE 1**  
**Smoke Yields for Flaming Combustion in Air from Tewarson [5]**

Material	Smoke Yield ( $g_{\text{smoke}}/g_{\text{fuel}}$ )	Comments
Gases and Liquids		
Ethyl alcohol	0.008	C—H—O
Ethane	0.013	C—H
Propane	0.024	C—H
Heptane	0.037	C—H
Propylene	0.095	C—H unsaturated
Acetylene	0.096	C—H unsaturated
Styrene	0.177	C—H aromatic
Toluene	0.178	C—H aromatic
Solids (Polymers)		
Teflon (PTFE)	0.003	C—F halogenated linear structure
Wood (red oak)	0.015	C—H—O structure
Polymethylmethacrylate (PMMA)	0.022	C—H—O structure
Polypropylene (PP)	0.059	C—H branched structure
Polyethylene (PE)	0.060	C—H linear structure
Nylon	0.075	C—H—O—N linear structure
Polyester (PET)	0.089–0.091	C—H—O aromatic structure
Polycarbonate (PC)	0.112	C—H—O aromatic structure
Rigid polyurethane (PU) foam	0.104–0.130	C—H—O—N aromatic structure
Flexible polyurethane (PU) foam	0.131–0.227	C—H—O—N aromatic structure
Polystyrene (PS)	0.164	C—H aromatic structure
Polyvinylchloride (PVC)	0.172	C—H—Cl halogenated linear structure

measurements of red oak and PMMA indicated that smoke yield was roughly equivalent for comparable specific burning rate [4].

Finally, the fire environment is an important factor. If the air flow is less than what is required for complete combustion (underventilated fires), the soot yield usually increases. Tewarson found that smoke generation efficiency for six materials under ventilation-controlled conditions increased by up to 2.8 times [7]. Measured smoke yields for wood cribs were found to be an order of magnitude larger under underventilated conditions than when well ventilated [8]. As mentioned in the previous section, the organic fraction of the smoke aerosol also increases for underventilated burning. Such smoke aerosol is likely to be more toxic than that produced during overventilated burning [9].

### **Fractal Morphology**

A key characteristic of the structure of the soot is its fractal character. This is evident in the power law dependence between the number  $N$  of primary spheres in an agglomerate and the radius of gyration,  $R_g$ , which is defined as the 2nd moment of the mass distribution:

$$N = C(R_g/r_p)^{D_f}, \quad (1)$$

where  $r_p$  is the radius of the primary spheres and  $D_f$  is the fractal dimension. The value of  $D_f$  often obtained by image analysis of transmission electron microscopy and light scattering is

found to be in the range of 1.70–1.85 [10–12]. Sorensen provides a comprehensive review [13] of measurements of fractal dimension of soot and also of the prefactor  $C$ . The fact that the dimension is less than two means that most of the primary spheres will be seen in a 2-D projection, and that as the agglomerate size increases the density of the particle decreases. This second feature leads to a particle settling velocity much smaller than a sphere with the same radius of gyration. In the 1980's there was active interest in computer simulation of the agglomerate growth using molecular dynamics based on the Langevin equation [14] and by Monte Carlo simulation [15, 16]. These studies involving cluster-cluster agglomeration resulted in fractal dimensions and optical structure factors, which are related to the Fourier transform of the cluster pair distribution function, similar to the experimental results. Later in this paper we will discuss particle growth processes that might affect the agglomerate size as the smoke moves through a building, as well as the key agglomerate properties for particle deposition in the respiratory track and for particle losses during transport.

### ***Aerodynamic Diameters and Size Distribution***

In a plot of frequency vs. size for smoke aerosols, the distribution is strongly skewed, with the number of smaller particles much greater than the number of larger ones. A Gaussian distribution is thus a poor fit to the data. Instead, smoke aerosols are often reasonably well represented by a log-normal particle size distribution function [17, 18]. In this type of size distribution, which provides certain mathematical advantages for particle size analysis [19], the logarithm of the diameter, rather than the diameter itself, satisfies a Gaussian number distribution. If  $n_i$  is the number of particles with diameter  $d_i$ , the mean geometric diameter  $d_g$  is given by:

$$\log d_g = \frac{\sum n_i \log d_i}{\sum n_i} \quad (2)$$

and the geometric standard deviation  $\sigma_g$  is:

$$\log \sigma_g = \left[ \frac{\sum n_i (\log d_g - \log d_i)^2}{\sum (n_i) - 1} \right]^{1/2}. \quad (3)$$

Note that the value of  $\sigma_g$  is dimensionless; instead of adding or subtracting from the mean diameter,  $\sigma_g$  is a multiplicative factor, with one geometric standard deviation representing a range of particle sizes from  $(d_g/\sigma_g)$  to  $(d_g \times \sigma_g)$  that contains 68.3% of all particles [20]. For a perfectly monodisperse distribution,  $\sigma_g = 1$ .

The average size of particles described by a log-normal size distribution function may be quantified by any of a large number of median and weighted mean diameters. The wider the size distribution, as measured by the geometric standard deviation, the larger the difference between various measures of average diameter [18]. Since smoke particle size distributions are typically quite broad, and since different experimental techniques measure different average diameters, it is critical to select the average diameter measure and measurement technique that best capture the information relevant to the specific problem at hand.

For the purpose of assessing health risk due to particle deposition in the respiratory tract, the most appropriate measure of size is the aerodynamic diameter [17]. This is defined as

the diameter of a unit density sphere (density =  $1 \text{ g/cm}^3$ ) having the same aerodynamic properties as the particle in question. In other words, the settling velocity of a particle of any shape or density with a given aerodynamic diameter is equal to that of a spherical water droplet of the same diameter [17, 18]. Two major mechanisms of particle deposition in the lungs are via sedimentation and impaction. In both cases the aerodynamic diameter is the characteristic diameter independent of particle shape.

A cascade impactor [17] is the apparatus most frequently used to measure aerodynamic diameter. In this device, the aerosol enters a compartment containing a series of collection platforms known as stages. Inertial forces transport particles in a direction perpendicular to the streamlines of the velocity field in this compartment with a rate dependent on flow field, size, and density, causing particles in successively smaller size ranges to impact on successive stages. The mass of particulate matter on each stage is plotted on a log scale as a cumulative distribution function. The mass median aerodynamic diameter is the 50% point on this curve, and the degree to which the size distribution is described by a log-normal distribution is established by how closely the curve represents a straight line. If the distribution is indeed log-normal, the geometric standard deviation is given by the particle size at the 50% probability point divided by the size at 15.9% probability [17, 18].

Size distribution data, including mass median aerodynamic diameter (MMAD) and standard deviations, are presented in Table 2 for smoke aerosols produced by flaming combustion. This data is presented graphically in Figure 1. The reported median aerodynamic diameter for smoke aerosols ranges from  $0.05 \mu\text{m}$  for flaming wood to  $10 \mu\text{m}$  for acetylene. For all fuels except acetylene at high flow rates, the MMAD is less than  $3.5 \mu\text{m}$ , and for a majority of the fuels most of the smoke aerosol is in the sub-micrometer range. Figure 1 illustrates a trend of aerodynamic diameter increasing as smoke yield increases.

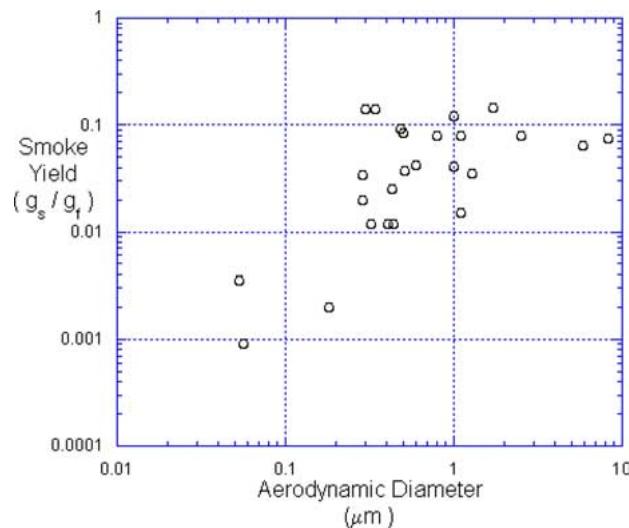


**Figure 1. Smoke yields and mass median aerodynamic diameters for flaming experiments listed in Table 2.**

**TABLE 2**  
**Size Distribution and Yield of Smoke Aerosols Produced During Flaming Combustion**

Fuel Type	Fuel Size (m <sup>2</sup> unless noted)	Smoke Yield (g <sub>smoke</sub> /g <sub>fuel</sub> )	Mass Median Aero. Diam. (μm)	Geom. Stand. Dev.	Comments	References
Heptane	3.5 mm diam. cotton wick bundle	NA		1.5		[67]
Acetylene	67.5 cc/min	0.062-0.088	6.4-9.6	No fit	Gas	[21]
	72 cc/min	0.064	5.8			[68]
	59.0 cc/min	NA	2.4, 3.8	No fit		[21]
	51.0 cc/min	NA	0.72	No fit		
	43.3 cc/min	0.029-0.042	0.43-0.59	8.5-14		[68]
Kerosene	42 cc/min		0.48			[21]
	39.5 cc/min	0.008-0.015	0.24-0.46	3.8-20	Pool fire	[69]
	0.09	NA	3.2	12-13		
Crude oil	0.36	NA	1.56, 0.57	11, 31		[6]
	1.13	0.12	1.0		Pool fire	[34]
	1.13	0.080	2.5	3.1	Aged 150 min	
			1.1	2.4	Aged 90 min	
Asphalt Douglas fir			0.8	2.7	Fresh	[70]
	0.28	0.085	0.5	6.8	Pool fire	[6]
	3.1	0.14	0.3			[8]
	2.27	0.14	0.34	8.5	Shingles, 30° angle	[8]
	0.411 m <sup>3</sup>	0.035	1.28	3.1	Wood crib, Undervent.	[8]
	0.006	0.025	0.43	2.37	Vert., 2.5 W/cm <sup>2</sup> , 4.8 l/s	[71]
	2.23	0.002	0.18	16	Plywood, Vert., Parallel plates	[8]
	0.137 m <sup>3</sup>	0.0009	0.056	46	Wood crib	

(Continued on next page.)

**TABLE 2  
(Continued).**

Fuel Type	Fuel Size (m <sup>2</sup> unless noted)	Smoke Yield (g <sub>smoke</sub> /g <sub>fuel</sub> )	Mass Median Aero. Diam. (μm)	Geom. Stand. Dev.	Comments	References
Birch wood	0.0225	0.0035	0.053	16	Vert., Parallel plates	[72]
Polymethyl methacrylate (PMMA)	0.006	0.015-0.018	1.1	9	Varied heating rate, airflow, %O <sub>2</sub>	[73]
Polystyrene	0.006	0.041	1.0	4	Varied heating rate, airflow, %O <sub>2</sub>	[73]
Polyvinyl chloride (PVC)	0.006	0.105-0.185	0.4-3	2.5-7	Varied heating rate, airflow, %O <sub>2</sub>	[73]
Rigid PVC	0.006	0.012	0.44	2.02	Vert., 2.5 W/cm <sup>2</sup> , 10% O <sub>2</sub>	[71]
		0.012	0.41	2.22	Same w/ air	
Polypropylene	0.006	0.042	0.6	11	Varied heating rate, airflow, %O <sub>2</sub>	[73]
Rigid polyurethane foam	0.006	0.091	0.48	1.90	Vert., 2.5 W/cm <sup>2</sup> , 7.2 l/s	[71]
Flexible polyurethane foam	0.0225	0.034	0.29	16	Horiz.	[72]
High density polyethylene (HDPE)	0.006	0.018-0.023	0.17-0.4	3-6	Varied heating rate, airflow	[73]

Flame-generated smoke agglomerates have a broad range of geometric standard deviations extending from 2 to 16 and even larger. Because of the complex shape of the agglomerates formed in the flame, there is a lack of an independent verification of the aerodynamic size distribution of these particles. Cleary [21] found for soot generated by burning acetylene as a laminar diffusion flame that the aerodynamic diameter was a factor 3 to 5 smaller than the overall agglomerate size. Cleary also reported that the nature of the impactor collection substrate affects the measurement of both the aerodynamic median diameter and the range of the distribution. A smooth surface such as aluminum foil, which was used in most of the studies reported in Table 2, leads to “particle bounce” and a smaller apparent particle size compared to the results with a surface coated with a greasy material.

There is a need for a better quantification of the aerodynamic properties of smoke agglomerates.

### **Changes in Smoke Aerosol due to Particle Transport and Decay**

A smoke aerosol is a dynamic entity in terms of its motion, the particle size distribution, and its chemical content. The gross motion of smoke is determined by the fluid mechanics of buoyancy-driven flow. To a large extent, the motion of the aerosol mimics that of the gas flow. However, there are smaller-scale transport processes affecting the concentration and size distribution of the particles. There are several processes leading to losses in the particle concentration including particle sedimentation, particle diffusion in the boundary layer region to the surface, and thermophoretic deposition from a hot smoke near a cooler surface. This section describes each phenomenon, provides the formula defining the transport property, and gives estimates for the amount of smoke deposited as a result of each process.

The particle size distribution can also change as a result of individual particles coagulating through collision and adhesion. The resulting increase in average particle size will affect the aerodynamic diameter and thus the amount deposited in various portions of the respiratory tract. Other growth processes are important for certain gaseous species. These include condensational growth and the adsorption of gases on the particle surfaces.

#### **Wall Loss**

Should there be significant loss of smoke particles at surfaces, the tenability of the fire environment could improve. There are three processes that can lead to wall losses: thermophoresis, sedimentation and diffusion.

*Thermophoresis.* Small particles in the gas phase are driven from high to low temperature regions. This becomes important in fires because the gas temperature as it impinges on the ceiling can be very high compared to the wall temperature. This is evident in fires by the black deposit on the ceiling directly above the fire with decreasing evidence for deposition as one goes out from the center. For particles much smaller than the mean free path of air, the thermophoretic velocity is independent of particle size and is given by the following equation [22]:

$$v_T = \frac{-0.55\eta}{\rho_g T} \frac{dT}{dx}, \quad (4)$$

where  $dT/dx$  is the temperature gradient and  $\eta$  and  $\rho_g$  are the viscosity and density of air respectively. In this limit the thermophoretic velocity in air for a temperature gradient of 100 K/cm is 0.03 cm/s. Where the particle size is large compared to the mean free path, the thermophoretic velocity depends on the thermal conductivity of both the gas and the particle [17]. The velocity is lower in this limit by a factor of 3 to 10 depending on the thermal conductivity of the particle. In the transition region between the free molecular region and the continuum, the thermophoretic velocity lies between these limiting values.

*Sedimentation.* The settling velocity of a particle is computed from the balance between the gravitational force and the drag force [17] leading to the equation:

$$v_s = \frac{\rho_p d^2 g C}{18\eta}, \quad (5)$$

where  $d$  is the particle diameter,  $\rho_p$  is particle density,  $g$  is acceleration due to gravity, and the Cunningham slip correction  $C$  accounts for non-continuum effects through the following expression:

$$C(d) = 1 + K_n[A_1 + A_2 \exp(-A_3/K_n)], \quad (6)$$

in which the Knudsen number is the mean free path in air divided by the particle radius ( $K_n = 2\lambda/d$ ), and constants are  $A_1 = 1.142$ ,  $A_2 = 0.558$ , and  $A_3 = 0.999$  [23].

*Diffusion.* Smoke particles undergo Brownian motion, manifested as random motion of the aerosol particles as a result of collisions with other particles. The Stokes-Einstein equation for the diffusion coefficient  $D$  is given by [17]

$$D = \frac{kTC}{3\pi\eta d}, \quad (7)$$

where  $k$  is Boltzmann's constant and  $C$  is the Cunningham slip correction.

*Relative Effects of Transport Processes.* Table 3 compares the magnitude of the wall loss effects for these three transport processes. We consider a uniformly distributed aerosol and a surface with a sticking boundary condition for the case of diffusion, aerosol settling on a surface for sedimentation deposition, and a fixed temperature gradient of 100 K/cm for the case of thermophoresis. In all cases, it is assumed that a particle touching the surface sticks. It is apparent that for the case of a 100 K/cm temperature gradient, thermophoresis results in a larger deposition rate than either of the other processes except for sedimentation of the largest particle sizes.

Factors that impose significant limitations to this type of calculation include turbulent flow effects and soot agglomeration.

The results in Table 3 assume a static flow, while realistic fire-driven flows are buoyant and turbulent. The general approximation made in realistic calculations of particle deposition is that the particle concentration in the turbulent flow is uniform until one approaches the boundary layer, where the concentration decreases linearly to the surface. The diffusion

**TABLE 3**  
**Comparison of Calculated Particle Deposition Modes**

Particle Diameter, $\mu\text{m}$	Thermophoresis	Diffusion	Sedimentation
0.01	$2.8 \times 10^6$	$2.6 \times 10^5$	$6.7 \times 10^2$
0.1	$2.0 \times 10^6$	$2.9 \times 10^4$	$8.6 \times 10^3$
1.0	$1.3 \times 10^6$	$5.9 \times 10^3$	$3.5 \times 10^5$
10.0	$7.8 \times 10^5$	$1.7 \times 10^3$	$3.1 \times 10^7$

Particles sticking to a  $1 \text{ cm}^2$  surface during a 100 s period for a suspended particle density of  $10^6$  particles/ $\text{cm}^3$ .

velocity  $v_D$  in this case is given by:

$$v_D = \frac{D}{\delta}, \quad (8)$$

where  $\delta$  is the boundary layer thickness. The rate of deposition is much greater for turbulent buoyant flow compared to diffusion in still air because of the much larger gradient near the surface for the turbulent flow. The difficulty in applying this analysis is in the determination of the boundary layer thickness. The thermal gradient driving the thermophoretic deposition will also have a boundary layer thickness that is typically much greater than the particle concentration boundary layer thickness.

The other serious difficulty in making a quantitative analysis for the case of flame-generated soot arises from its complex particle shape. The particle deposition rates in Table 3 are for spherical particles. There is some evidence that Eq. (4) for the thermophoretic velocity of particles small compared to the mean free path also applies to soot agglomerates. The qualitative reason for this simplification is that both the thermophoretic force acting on the particle and the drag force are proportional to the number of primary particles in the agglomerate for fractal dimensions less than 2. The thermophoretic velocity is obtained by equating these two forces, and the dependence on the number of primary spheres cancels out. There is experimental evidence based on opposed flow diffusion flames that is consistent with this result [24], but quantitative data is lacking for larger post-flame agglomerates. Since the cascade impactor measures the aerodynamic diameter, there is data on the aerodynamic diameter, such as that in Table 2, from which the settling velocity can be estimated. It would still be of value to do sedimentation experiments to verify that the flow through the impactor orifices does not change the structure of the agglomerates. Several studies [25–27] have been performed on the diffusive mobility of soot agglomerates. Wang et al. [25] have developed a method for correlating the existing data for a range of Knudsen numbers, extending from about 20 corresponding to in-flame conditions for small agglomerates to about 0.03 for post-flame conditions for large agglomerates. There is still a need for more quantitative measurements of the diffusion coefficient of well-characterized soot agglomerates.

*Experimental Data.* For room fires, there are no quantitative data on the soot deposited within the enclosure or in the connecting corridor and adjacent rooms. Lacking such information, we rely on a variety of studies providing deposition rate information for conditions

simulating some of the features of smoke deposition in a room fire to provide an estimate of the magnitude of the action of the smoke deposited. In a study by Dobbins et al. [28], smoke from burning crude oil was collected in a hood above the fire and drawn into a 1 m<sup>3</sup> aging chamber. The initial temperature of the soot was about 100°C, and it cooled to within a few degrees of the walls in a few minutes. The mass concentration of the smoke was monitored over a period of 90 min. There was about a 10% decrease in the aerosol mass concentration in 15 min and about 25% over a period of 90 min. The dominant particle deposition mechanisms in this case were sedimentation and diffusion with a small effect from thermophoresis when the smoke first entered the chamber. If the experiment were scaled up to the size of a realistic enclosure, the deposition via diffusion and sedimentation would be less because of the smaller surface area per unit volume.

Eventually, theoretical analysis of thermophoretic deposition may provide a simplification in predicting deposition for realistic conditions. For a flow of a particle-laden gas toward a cold isothermal surface, Batchelor and Shen [29] found for a range of flow conditions that the particle deposition is proportional to the heat flux to the boundary. Rosner et al. [30] have made a general analysis of the effects of heat transfer on the dynamics and transport of small particles. The capability to compute the convective heat transport from a buoyant plume to the ceiling and walls of an enclosure for a 3-dimensional transient boundary layer is just now being developed by Baum and Rouson [31]. Combining this model with the particle transport analysis [24, 30] could allow the computation of the thermophoretic deposition of the smoke to the walls and ceiling at the same time that the convective heat transport is computed.

A study by Mulholland et al. [4] provides a sense of the magnitude of the thermophoretic deposition. Smoke generated using the Cone Calorimeter apparatus was drawn through a 6.3 mm diameter stainless steel tube. The inlet temperature of the smoke,  $T_i$ , was in the range of 450 K to 625 K with an outlet temperature  $T_o$  of 300 K. It was found that the deposited fraction of smoke,  $f_T$ , was approximately proportional to the ratio of the temperature difference to the inlet temperature:

$$f_T = 0.5 \frac{T_i - T_o}{T_i}. \quad (9)$$

Qualitatively, this expression suggests that the particle deposition is proportional to the heat loss even in the case where the wall temperature is not isothermal.

We can make an upper bound estimate of the thermophoretic deposition from a hot smoke layer by using Eq. (9) with the assumption that the gas changes temperature solely through convective heat exchange with the ceiling. We assume that the initial ceiling temperature is 1300 K and the temperature leaving the building is 300 K. For these assumptions, we compute  $f_T = 0.38$ . A more realistic assumption is that only half of the heat transfer is to the ceiling while the other half is to the entrained flow beneath the ceiling layer. This results in a value of 0.19 for  $f_T$ .

The rough estimates given above suggest that about 10% to 30% of the smoke produced would be deposited within the room containing the fire over a period of 10 min to 30 min. The value could be less than this if the fire were small or could be larger if the fuel produces very large soot agglomerates such as is the case with polystyrene. The deposition over a

long period could be larger if there is very little flow into or out of the enclosure such as the case with a closed door.

### **Smoke Coagulation/Agglomeration**

Changes in the size of smoke particles affect their movement toward surfaces and their surface area, which in turn affects the mass of toxicants they can transport. Smoke aerosols are dynamic with respect to their size distribution function. Smoke particles or droplets undergoing Brownian motion collide and stick together, leading to the formation of agglomerates. The coagulation equation expresses the rate of change in the concentration for a given particle size as a second order kinetic process involving gains due to collisions of two agglomerates to form a larger agglomerate and losses resulting from an agglomerate with a specified number of primary spheres colliding with any other agglomerate [32]. Integrating the coagulation equation over all particle sizes assuming a size-independent coagulation coefficient  $\Gamma$  leads to an equation for the rate of change of the total number concentration  $N$ :

$$\frac{dN}{dt} = -\Gamma N^2. \quad (10)$$

The value of the coagulation coefficient was estimated to be  $1.0 \times 10^{-9}$  for smoke from flaming  $\alpha$ -cellulose [33] and  $1.5 \times 10^{-9}$  for smoke produced by the burning of crude oil [28]. Integrating equation (10), we obtain an expression for the total number concentration as a function of time based on a homogeneously distributed aerosol with initial total number concentration  $N_0$ :

$$N = \frac{N_0}{1 + \Gamma N_0 t}. \quad (11)$$

The total number concentration within a flame is on the order of  $10^9$  particles/cm<sup>3</sup> to  $10^{10}$  particles/cm<sup>3</sup>, and the coagulation coefficient is greater than the values given above because of the increased temperature. Assuming a number concentration of  $10^{10}$  particles/cm<sup>3</sup> and a coagulation coefficient of  $5 \times 10^{-9}$ , one finds based on Eq. (11) that the number concentration has decreased by a factor of 26 after 0.5 s residence time in the flame. This suggests that there would be a significant amount of agglomeration within the flame. Agglomerates with as many as 100 spheres have been observed by transmission electron microscopy for soot sampled thermophoretically within the flame.

The equation above applies to a uniformly distributed smoke aerosol, while smoke produced by a fire is being continuously diluted by the entrainment of air. There is a lack of direct experimental data on the effect of the coagulation process on the size distribution of the smoke as the smoke travels from near the fire to a remote location where it might be inhaled by someone escaping the fire. If the smoke particle size increases by a large amount during this trip, this may mean that less of the smoke will penetrate deep into the respiratory system.

The smoke aging study carried out by Dobbins et al. [28] provides insight regarding the coagulation process. The smoke from a crude oil pool fire was collected in a hood about 2 m above the base of the fire and then sampled into a 1 m<sup>3</sup> aging chamber. The

temperature (100°C) and concentration (100 mg/m<sup>3</sup>, 6 × 10<sup>6</sup> particles/cm<sup>3</sup>) of the smoke entering the chamber are estimated to be similar to what the smoke properties would be for the plume as it reaches the ceiling of a room. Over a 90-min period, it was found that the smoke number concentration decreased by a factor of 24 during which time the mass concentration decreased by only 25%. From these concentrations and assuming a density of 2 g/cm<sup>3</sup> for soot, we compute that the diameter of average mass increases from 0.25 μm to 0.72 μm. The aerodynamic mass median diameter increased from 0.8 μm to 1.1 μm during this same aging period, as shown in Table 2 [34]. The reason for the relatively small change in the aerodynamic diameter is the broadness of the size distribution, resulting in a peak in the number distribution about a factor 4 lower than the peak in the mass distribution. Coagulation of small particles with each other has a large effect on the number concentration and on the count median size, but coagulation of a small particle or agglomerate with a large agglomerate has little effect on the mass of the large particle. The example given here is probably an overestimate for the effect of coagulation on the aerodynamic diameter, since in a more realistic scenario the smoke would be diluted by entrained air.

The above scenario suggests that there may not be a large change in the mass median aerodynamic diameter as a result of coagulation for an enclosure fire from the time the smoke aerosol leaves the room of fire origin until it reaches another location. Thus, if the initial size distribution indicates a large fraction of respirable particles, this will still be true for the aged particles some distance from the fire.

The agglomeration process is most effective at reducing the concentration of the smallest clusters or small spheres by large agglomerates. The particle coagulation coefficient involves a product of the effective collision cross-section and the particle diffusion coefficient. Both of these terms are large for collisions between a large particle and a small particle because of the large collision cross-section of the large agglomerate and the large diffusion coefficient of the small agglomerate. The implication of this process in removing very small particles produced by the burning of PTFE will be discussed in a later section.

While the above analysis suggests that coagulation may have only a small effect on the aerodynamic mass median diameter, this result is based on a limited data set for a single fuel burning at a fixed heat release rate. It would be valuable to measure the size distribution of smoke collected at various regions in a multi-room test facility for a range of burning materials and fire sizes to assess the effect of aging on the size distribution.

## **Adsorption and Desorption of Toxic Gases on Smoke Particles**

The preceding sections considered the state of knowledge of characteristics of particles produced in a fire and their transport through the fire environment. In this section we consider the question of the type and quantity of toxic gases that are likely to be carried and deposited in the respiratory tract as a result of being adsorbed on the smoke particles or water droplets. The topic of nanoparticle toxicity is also discussed in the context of smoke.

Gas adsorption relates to the transport of gas to a surface and the attachment to the surface through physical or chemical interactions. In thermodynamic equilibrium for a specified gas adsorbed on a specified solid at a fixed temperature, the quantity of gas taken up by the surface is a function of its pressure,  $n = f(p)$ , or relative pressure,  $n = f(p/p^0)$ ,

where  $p^0$  is the saturation vapor pressure of the adsorbate [35]. This relationship, known as an isotherm, has played a central role in the development of models for adsorption and the understanding of adsorption mechanisms. Even though a fire environment is not in equilibrium as a system, it is still a good approximation at the scale of vapor adsorbing on a particle.

During adsorption, unsaturated forces at the surface of a condensed phase material, the adsorbent, are at least partially saturated by interactions with gas-phase molecules, the adsorbate [36]. Two types of adsorption are distinguished by chemical versus physical bonding.

- *Chemisorption* refers to the formation of a true chemical bond between the adsorbate molecule and the surface of the adsorbent. The process is strongly exothermic, releasing in excess of 0.5 eV per adsorbate molecule, but the energy barrier in breaking existing chemical bonds within the gas molecule or surface structure or both must first be overcome.
- In *physisorption*, the interaction between gas molecules and surface is controlled by weaker electrostatic or van der Waals forces, the same forces as those involved in condensation. Since no energy barrier exists, physisorption is reversible and occurs over a much more rapid time scale than chemisorption.

There are also intermediate classes of bonding including dipole interactions, multi-layer bonding, and hydrogen bonding.

Desorption, the removal of the gas molecule from the condensed phase smoke particle surface, is an endothermic process that occurs to some extent for all types of bonding except chemisorption. The deposition of toxic gases in the respiratory tract after transport by smoke molecules depends on the bonding of the gas to the particle and on the surface forces exerted by the respiratory tract tissue on the molecules adsorbed on the smoke particle.

### ***Soot Surface Effects***

A good review of the field of surface adsorption is provided by Rudziński et al. [37]. Adsorption processes for soot have been the subject of considerable recent research because of concerns about the effects of man-made particulates on atmospheric chemistry and human health. Soot particle surfaces are highly complex due to both the wide variety of surface chemical functionalities and their agglomerate physical structures, which result in large surface areas. Their strong affinity for gases of many kinds has long been noted, with many industrial processes employing specially-designed “activated carbons” to remove impurities and act as reducing agents.

Considerable research has been done on the adsorption properties of carbon blacks and activated carbon. Care must be taken in projecting those results to adsorption on naturally-occurring smoke, however, since the engineering of these commercial products has modified their chemical and physical properties significantly. Both carbon black and activated carbon have considerably larger surface areas, due to the rapid cooling of soot to produce carbon black [38] and to the dehydration, carbonization, and activation processes that create the extensive network of pores in activated carbon [39]. In addition, mineral matter is incorporated into commercial activated carbons to improve reactivity, and surface properties such as polarity and pore size are designed to optimize adsorption.

Particulate characteristics affecting the rate and extent of adsorption include: (1) surface functional groups and (2) pore structure.

*Surface Functional Groups.* Carbonaceous aerosols formed by combustion processes vary widely in their surface properties depending on their origins, thermal history, and the composition of the surrounding environment as they form and develop. The range of responses of soot particles to hydration, for example, is due to differences in chemistry during soot development [40]. Subsequent surface oxidation of a soot particle during aging increases the acidity and polarity of the carbonaceous surface, probably due to the formation of carboxylic acid groups, making the surface more hydrophilic with time. Physisorbed O<sub>2</sub> and incorporation of trace elements such as sulfur increase soot hydration as well [41].

The chemical content of soot may include elemental carbon (graphite), organic matter from incompletely-burned fuel, and other elements derived from the burning object such as nitrogen from polyurethane. Soot consists of randomly oriented graphitic microcrystallites, or platelets. The most chemically reactive areas are likely to be at the edges of these platelets [40]. Along the edges, where aliphatic and aromatic chains are exposed, highly reactive sites may be found where carbon is not exerting its full valency of four bonds and is attached to other atoms with only three bonds. Only a percentage of the carbonaceous surface is active. For example, coverage of the surface by oxygen-containing functional groups has been measured at about 50% for *n*-hexane soot [41]. While the maximum adsorptive capacity of a particle is largely determined by its surface area, the surface functionalities, which are specific to the type of fuel and combustion history, are important at lower adsorbate partial pressures [38, 42].

*Pore Structure.* The adsorption properties of a soot particle are also affected by its porous structure. Pores are classified in three basic size ranges. Macropores, with pore width greater than 50 nm, provide access into the interior of the particle. Mesopores, with pore width in the range of 2 nm to 50 nm, are of the proper size for the formation of a meniscus of the liquefied adsorbate, and therefore provide sites where capillary condensation may take place. Pore sizes larger than about 10 nm are in part a result of primary sphere sizes on the order of 30 nm to 50 nm for the soot agglomerates. Micropore widths are under 2 nm and can represent a large fraction of the surface area available for adsorption. This category is further divided into supermicropores, from 0.7 nm to 2.0 nm, and ultramicropores, less than 0.7 nm in width [40, 43], compared to a molecular dimension of about 0.2 to 0.4 nm.

Information on the characteristics of the porous structure of real materials can be obtained from the shape of the measured gas adsorption isotherm, a plot of adsorbed amount versus relative pressure. An isotherm generally falls into one of five classes [35, 44]. For a nonporous solid, gas adsorption follows a Type II isotherm, in which the quantity adsorbed increases rapidly with relative pressure. After a monolayer has formed, the slope of the plot decreases, then gradually increases again as multilayers build up. The presence of micropores in the solid causes increased adsorption at low relative pressures due to the interactions of these sites followed by a leveling of the plot as adsorption sites fill, resulting in a Type I isotherm. The presence of mesospheres results in capillary condensation at higher relative pressures, increasing the adsorption over that of a nonporous surface and causing hysteresis in adsorption and desorption processes (Types IV and V). A small slope of adsorbed gas vs. low relative pressure (Types III and V) indicates that the adsorbent-adsorbate interaction is particularly weak.

Micropores less than 2 nm were found by Jaroniec and Choma [45] to play an important role in the surface adsorption of benzene on activated carbon by a factor of 10 or more times that of water. It is of interest whether soots also display this enhanced adsorption and whether it also occurs for other organics such as acrolein. The authors also report a high degree of surface irregularity for the activated carbons with a fractal dimension of about 2.6. The increase over a spherical surface exponent of 2 is mainly attributed to the micropore structure.

### ***Adsorbate Gas Effects***

The adsorption of a particular gas onto a soot particle is strongly dependent on the properties of the gas molecules.

*Polar Molecules.* In the case of polar molecules (e.g., H<sub>2</sub>O, HF, HCl, HBr, CO, NH<sub>3</sub>, NO, and HCHO), atom electronegativity and molecular structure result in a molecular dipole moment. Such molecules are preferentially adsorbed by sites with unpaired electrons and by acidic oxide groups. In addition to the weaker van der Waals forces that control the physisorption of non-polar molecules, polar molecules are likely to be held by hydrogen bonding [42]. Also, molecules with high dipole moments are preferentially adsorbed over, and may even displace, those with smaller dipole moments [40, 41]. This factor is of particular importance in the presence of highly polar water molecules, which is discussed in more detail below.

*Paramagnetic Molecules.* Paramagnetic molecules such as O<sub>2</sub>, NO<sub>2</sub>, and NO have unpaired electrons with parallel spins. Since many chemical functionalities on the soot particle surface also contain unpaired electrons, the attraction of this type of adsorbate molecule to these sites will be strong. The presence of paramagnetic molecules in the soot environment is expected to affect the adsorption properties of the soot toward other adsorbates, at least for those that may be adsorbed by these same sites. Study of the soot adsorption of these gases in combination with other diamagnetic or paramagnetic gases has provided insights into the coadsorption of multiple adsorbates [46].

*Aromatic Molecules.* Aromatic adsorbates, such as benzene and toluene, interact most strongly with carbonyl groups (carbon-oxygen double bond) on the soot surface [40]. The affinity of aromatic adsorbates is enhanced by an increase in the number of carbonyl groups, such as through soot aging, and decreased by acidic surface oxides.

*Other Organic Compounds.* Non-polar paraffinic compounds are hydrophobic in nature and adsorb preferentially on carbonaceous surfaces free from acidic surface oxides [40]. Such surfaces preferentially adsorb hydrocarbon vapors relative to water vapor [41]. Unsaturated organic compounds are preferred to saturated compounds on polar surfaces [39].

### ***Soot Hydration***

Hydration of soot particles from adsorption of water molecules already present in the atmosphere, generated in the fire, or introduced during suppression is a cooperative process. The more H<sub>2</sub>O molecules adsorbed, the stronger is the surface attraction toward additional H<sub>2</sub>O molecules [38]. If water were adsorbed onto the surface of a soot particle in sufficient quantities to change the local surface appearance to that of a water droplet, its adsorption properties with respect to other gases would be quite different.

Chughtai et al. [38] used the following expression to describe the mass of water adsorbed per gram of soot  $a$  as a function of humidity  $\rho/\rho_0$  for a variety of soots and carbon blacks:

$$\log a = \log a_0 - D[\log(\rho_0/\rho)]^2 \quad (12)$$

This equation applies for  $\rho/\rho_0$  up to about 0.55 and allows determination of the chemisorption limit, soot surface coverage at that limit, and the onset of multilayer formation. For the soots tested, chemisorption takes place at low relative humidities up to about 25%. The corresponding limiting surface coverages range from 6% to 18% for pine needle, *n*-hexane, coal, JP-8 (aviation fuel), and diesel fuel soots, reflecting the density of surface sites for irreversible adsorption of H<sub>2</sub>O (oxygen-containing surface functionalities) for each soot. For  $\rho/\rho_0$  between 25% and 55%, the dominant mechanism is quasi-reversible adsorption possibly facilitated by hydrogen bonding between surface sites, and for  $\rho/\rho_0$  from about 55% to 83%, multi-layer adsorption dominates through the cooperative interaction between adsorbed and gas phase molecules, again through hydrogen bonding.

Even at 83% relative humidity, the mass of water adsorbed per gram of soot is only in the range of 0.02 g H<sub>2</sub>O/g soot to 0.06 g H<sub>2</sub>O/g soot for natural soots. For liquid water to play an important role in transporting HCl to the alveolar region of the lungs, the mass of water must be comparable to the mass of smoke rather than only a small fraction of it.

Under certain conditions the humidity in the fire environment may be quite high, even saturated. The concentration of water vapor in a fire plume can be as large as a volume fraction of 0.1. The smoke plume cools as a result of thermal radiation, heat loss to the ceiling and walls, and entrainment of cool air. If the humidity of the ambient air is near 100%, which corresponds to a volume fraction of water vapor of about 0.03 at room temperature, it is possible that a water droplet cloud can occur from the condensation of water vapor on the soot. A supersaturation of a couple percent is adequate for the condensation to occur.

Mikhailov et al. [47] studied the hygroscopicity of soot aerosol in a chamber at 95%  $\pm$  2% relative humidity containing water droplets. While some coagulation of soot and water droplets occurred, the size distribution of the pure carbon soot aerosol did not change appreciably on exposure to the water droplets. For soot treated to increase the hydrophilicity of its surface, however, the mean size decreased by a factor of three. This is attributed to the compaction of wettable soot particles by capillary forces and subsequent water evaporation. More work is needed to verify that adsorbed water on soot in real fires does not increase markedly for saturated conditions.

### ***Transport of Specific Toxic Gases***

Table 4 contains a list of toxic gases that may be transported by smoke particles and some common materials that produce them during combustion. It also indicates the magnitudes of inhalation exposures that can cause sublethal effects ranging from significant sensory irritation to lung edema. Higher exposures can be fatal. Missing from Table 4 are CO and CO<sub>2</sub>. Although these are significant components of the fire gases, it is unlikely that smoke transport will play a significant role compared to the gas phase transport, because the gas phase concentration can far exceed the mass concentration of the smoke. Also, these molecules lack the polarity, solubility, and other molecular features needed for adsorption

**TABLE 4**  
**Major Transportable Toxic Gases from Combustion**

Toxic Gas	Potential Sources	Sublethal Effects
Acrolein (CH <sub>2</sub> =CHCHO)	Cellulosic materials, e.g., wood, cotton, paper; polystyrenes, ABS	A
Toluene diisocyanate (TDI)	Flexible polyurethane foams	A
Formaldehyde (HCHO)	POM, polypropylenes	B
Hydrogen cyanide (HCN)	Nitrogen-containing materials, e.g., wool, silk, PAN, ABS, acrylic fibers, nylons, urea/formaldehyde, melamine, polyurethanes, polyacrylamide	C
Nitrogen dioxide (NO <sub>2</sub> )	Nitrogen-containing materials	B
Hydrogen chloride (HCl)	PVC and chlorinated additives	B, D
Hydrogen fluoride (HF)	PTFE, other fluorinated compounds and additives	B
Hydrogen bromide (HBr)	Brominated compounds and additives	B, D
Sulfur dioxide (SO <sub>2</sub> )	Sulfur-containing materials, e.g., wool, vulcanized rubbers, poly(phenylene sulfide)	B
Hydrogen sulfide (H <sub>2</sub> S)	Sulfur-containing materials	C
Ammonia (NH <sub>3</sub> )	Nitrogen-containing materials	C
Styrene (C <sub>8</sub> H <sub>8</sub> )	Polystyrenes, ABS	C
Toluene (C <sub>7</sub> H <sub>8</sub> )	Polystyrenes, PVC, polyurethane foams	D
Benzene (C <sub>6</sub> H <sub>6</sub> )	Polystyrenes, PVC, polyesters, nylons	C

Sublethal effects occurring: A, below 10<sup>-5</sup> volume fraction (10 ppm by volume); B, 10<sup>-5</sup> to 10<sup>-4</sup> volume fraction (tens of ppm by volume); C, at 10<sup>-4</sup> to 10<sup>-3</sup> volume fraction (hundreds of ppm by volume); D, at 10<sup>-3</sup> to 10<sup>-2</sup> volume fraction (thousands of ppm by volume) [74].

of a large mass onto the soot. All of the gases in Table 4 are irritants except HCN, which is an asphyxiant.

Despite the awareness of the importance of aerosols in affecting smoke toxicity, there is relatively little quantitative information regarding the transport on particles of sufficient mass of noxious molecules to cause toxicological effects. The following summarizes the available information, the best of which is for HCl, with only limited data on HCN and other toxicants.

*Hydrogen Chloride.* The transport of HCl has been studied largely because it is a major pyrolysis and combustion product of polyvinylchloride (PVC), a polymer in widespread use. Chlorine is also present in a number of flame retardant additives. Further, other halogens (bromine and fluorine) are present in a number of commercial products, whose combustion generates the analogous halogen acids, HBr and HF. The transport for HBr should behave much like HCl; however, since HF is a weak acid due to the strong H-F bond, it is expected to penetrate farther in the respiratory tract. Still, HCl may be considered a surrogate for any toxic combustion product with high polarity and high solubility in water.

**Wall Losses for HCl.** For soot, the dominant mechanism for particle loss was thermophoresis. For gases such as HCl, the dominant mechanism is diffusion. It is important to be able to estimate the deposition of HCl to the walls to determine the gas and particle phase concentration of HCl transported away from the fire. Galloway and Hirschler [48]

have developed a five parameter model to predict the adsorption of HCl vapor on a variety of surfaces. The model includes a bulk gas phase, a boundary layer with a mass transfer rate of the HCl across the boundary layer, equilibrium between the gas phase concentration and surface concentration, and first-order reaction with the surface. The values of the mass transfer coefficients for the ceiling and walls were obtained from Cooper's analysis of the convective heat transfer to ceilings above enclosure fires together with the Reynolds analogy between heat and mass transfer [49]. Once the parameters were determined empirically, the measured and predicted concentrations of HCl concentration for a wide range of surface-to-volume ratios and different kinds of flow agreed to within about 20% in all cases reported, and often agreed within the measurement uncertainty. This model was incorporated within FAST [50] to describe the surface adsorption of HCl for large-scale experiments.

For one set of experiments involving a room and a corridor [51], agreement between experiment and model prediction of the remaining gas-phase HCl concentration was typically within about 20%. The amount of HCl deposited was about 25% for the 50 kW fire and about 15% for the 200 kW fire.

A second set of experiments involved a room, a corridor, and a target room where the concentration was monitored in the second room [52]. The agreement between measurement and prediction was about 30%. In this case, the deposition was much greater, ranging from 60% to 85%. This is due to the much smaller fire size (10 kW) together with the lower velocity for a "dead-end" flow into a second room compared to a flow through a corridor.

The full-scale tests demonstrate the sensitivity of the HCl loss to the details of the configuration and the fire size. It appears that the general approach used by Galloway and Hirschler could be applied for determining the parameters for other gases and then used to estimate the losses in full-scale tests. Such a study could incorporate the adsorption model into a field model for the smoke dynamics such as the Fire Dynamics Simulator developed by McGrattan and Forney [53].

**HCl Adsorption on Smoke Particles.** In order to transport HCl into the alveolar regions of the lungs and deposit it there, the molecule must be loosely bound to a smoke particle. To determine the partition of HCl gas molecules among those remaining in the gas phase, those bonded weakly to soot particles through physisorption, and those bonded tightly, or chemisorbed, Stone et al. [54] analyzed smoke products from combustion of cylinders of PVC film interleaved with sheets of polyethylene (PE). Nearly all chloride (98.4%) was found in the gas phase, 0.7% was easily desorbed from the soot during a 22 h purge, and 0.9% was tightly bound to the soot. This corresponds to about 20 mg of physisorbed HCl per gram of soot for a gas phase HCl volume fraction of  $2.7 \times 10^{-3}$  (2700 ppm by volume).

The quantity of physisorbed HCl provides another demonstration of the affinity of HCl gas for water. A comparison of the measured surface area of soot particles from this experiment with the  $0.15 \text{ nm}^2$  covered by a single HCl molecule suggests that HCl coats each particle to a depth of 1.5 monolayers. This thick coating is best explained by mixed adsorption of water vapor and HCl together by the soot.

The authors also estimated the amount of HCl that may be deposited within the alveolar regions of the lungs. Assuming that the density of soot is equivalent to the aerosol in this experiment at  $1.57 \text{ g/m}^3$ , that 40% of soot particles travel into the alveolar sacs, and that the breathing rate is 18 L/min over an exposure time of 1 h, the mass of HCl retained in the

lower lungs would be 13 mg [54]. This is equivalent to inhaling a volume fraction of about  $1 \times 10^{-5}$  HCl into the lungs for one hour and having it all be deposited.

Inhalation of smoke and gases from a fire containing halogenated materials is therefore expected to result in significant irritation to the upper respiratory tract from HCl gas with transport of a relatively small amount of HCl into the alveolar regions of the lungs by small soot particles.

**HCl Solution in Water Droplets.** Soot is not the only smoke particulate with the potential to transport HCl deeply into the lungs. Since HCl gas is highly water-soluble, it could also attach to small water droplets. To determine the fraction of HCl that could be transported by a water aerosol, Stone [55] set up a flow of HCl gas through a wetted wall tube of dimensions similar to those of the upper respiratory tract. The effect of a water aerosol stream on the transport of HCl through the tube was determined by comparing the amount of chloride deposited in the liquid film layer when the aerosol is present to that when it is not. A roughly even partition of HCl between gas phase and aerosol was found. Stone estimated that water droplets of  $3 \mu\text{m}$  or less in diameter are nine times as effective as soot in transporting HCl into the lungs.

This finding suggests that measurements are needed of the number and size distribution of water aerosols produced during fires. These are difficult measurements to make, but they would put the contribution of particle-borne acid gases in perspective.

*HCN.* Stone and Williams applied the same apparatus used to investigate HCl transport to consider the possibility that HCN could be transported into the lungs by a water aerosol [56]. The difference in the amount of HCN measured in the gas phase with and without the aerosol stream was negligible, indicating that the amount of HCN carried on the water droplets was under 1%. Water aerosol transport of HCN into the lungs would therefore not be a primary concern.

*Other Toxic Gases.* The main focus of most studies of adsorption of gases onto soot particles is on the effects of atmospheric particulates on human health and the environment. Much research has been done on gases such as CO, CO<sub>2</sub>, O<sub>2</sub>, NH<sub>3</sub>, NO<sub>2</sub>, NO, and other NO<sub>x</sub>, PAH, and SO<sub>2</sub>, but the adsorption of other gases of particular concern in fires, such as acrolein and TDI, has not been studied. Chughtai et al. [46] have studied the adsorption and reaction of a variety of molecular species found in the atmosphere on the surface of soot. Their analysis methods include microgravimetry and electron paramagnetic resonance (EPR). Table 5 displays results for some gases of interest during combustion. The adsorption of SO<sub>2</sub> and NO<sub>2</sub> for gas concentrations on the order of 0.2 volume percent is approximately 0.01 g of gas per g of soot, indicating that surface adsorption of such gases is negligible. The ability to distinguish different modes of surface adsorption for NO<sub>2</sub> compared to SO<sub>2</sub> from the EPR indicate that the SO<sub>2</sub> is primarily physisorbed while NO<sub>2</sub> is primarily chemisorbed.

### ***Toxicity of Ultrafine Particles***

Ultrafine particles are defined as having an aerodynamic equivalent diameter less than  $0.1 \mu\text{m}$ . Ultrafine particles with diameters of about  $0.03 \mu\text{m}$  and smaller have been found to cause an inflammatory response in the respiratory system not seen with fine particles about

**TABLE 5**  
**Gas Adsorbate Data: from Chughtai et al. [46]**

Adsorbate	Polar Molecule	Para- or Dia-magnetic	% Chemisorbed	% Physisorbed	Temp.	Comments
NO <sub>2</sub>	Weak	P	90.3	9.7	22 °C	1010 ppm NO <sub>2</sub> , 15 mg soot
NO	Weak	P	0	100		
NH <sub>3</sub>	Moderate	D	100	0		17, 34, 57, 68 ppm NH <sub>3</sub> w/20 mg soot 34 ppm NH <sub>3</sub> w/5, 10, 15, 20 mg soot 0.21 mg NH <sub>3</sub> /g soot, surface coverage 1.2
SO <sub>2</sub>	Moderate	D	17.7	82.3	22 °C	1010 ppm SO <sub>2</sub> , 15 mg soot,
			19.0	81.0	34 °C	surface coverage 8.58, 6.84,
			22.8	77.2	46 °C	4.79, 2.25
			23.7	76.3	66 °C	

0.25  $\mu\text{m}$  in diameter, even though the material itself is inherently nontoxic [57]. For particles with intrinsic toxicity, the cell damage and release of inflammatory mediators is much greater for ultrafine than for larger particles. Epidemiological studies also indicate a link between the smallest particulate sizes and adverse effects on cardiopulmonary health [58]. Although the mechanisms of damage are not yet completely understood, recent research has provided some insights.

The lung damage mediated by ultrafine particles is hypothesized to result from the penetration of these particles into the interstitium in the alveolar regions of the lungs [57]. In this scenario, particles travel into the alveoli, where they overcome the capability of the macrophages to clear the lungs by engulfing foreign material and ingesting it or transporting it to the mucociliary escalator for removal. This may occur due to injury to the macrophage cells themselves, to particle numbers that overload the system [57], or to contamination of the pulmonary surfactant [59]. Ultrafine particles that escape the macrophages are small enough to pass through the epithelium into the interstitium, where it is hypothesized that they may act as a chronic irritant to cells or be transported to the lymph nodes. This damage may occur even for particles that are chemically inert, as has been seen in experiments with ultrafine particles of TiO<sub>2</sub> and carbon black [60].

There is one type of combustible material for which the issue of smoke toxicity due to ultrafine particles has been raised. Under experimental conditions, the vapors from combustion of pure perfluoropolymers (PFP), such as polytetrafluoroethylene (PTFE) and tetrafluoroethylene-hexafluoropropylene copolymer (FEP) were found to manifest toxic potency up to a thousand times that of the combustion gases from other materials or PTFE in other toxicity tests. In a small-scale combustion toxicity test, rats were found to die from 30 min exposure to as little as 0.04 mg of PTFE combustion products per liter [61], as compared to a 30 min LC<sub>50</sub> of 3.8 mg/l for CO gas and 20 mg/l to 50 mg/l for combustion products from woods and most plastics. Further testing established that the lethality of these fumes was significantly reduced or eliminated by aging, filtering, and co-combustion products with other materials, and that the high toxic potency could be restored during the aging process by reheating [9, 62, 63]. These results pointed to ultrafine monodisperse

particulates as a causal factor. Measurements of highly toxic PFP aerosols showed that a significant number of particles are  $0.02 \mu\text{m}$  in diameter or smaller, presumably formed by condensation of a dilute vapor of relatively low molecular weight fluoropolymer [64]. Experiments with rats show that PTFE fumes containing ultrafine particles cause severe inflammatory damage involving pulmonary macrophages and epithelial cells [65]. As the PFP aerosol cools and ages, however, or in the presence of a dense particle concentration, thermal coagulation of these primary particles causes the formation of much larger aggregates, and the high toxic potency is eliminated. The complexity of this research area is further demonstrated by recent results by Johnston et al. [66] that neither PTFE particles denuded of the gas phase species by generation in argon nor the gas phase species with particles removed by filtration are highly toxic. This suggests a role for surface chemistry or adsorbed reactive gases.

### Summary

- Most of the initial smoke aerosol is in the size range for effective transport to the alveolar regions of the respiratory tract. Flaming combustion produces soot agglomerates with mass median aerodynamic diameters of approximately  $0.5 \mu\text{m}$ .
  - “Ultrafine” particles with a diameter of  $0.02 \mu\text{m}$  and less may be much more toxic than particles with a larger diameter.
- Smoke yield, the mass of smoke generated for a given mass of fuel burned, varies from a fraction of a percent to 20% of the fuel mass. Flaming combustion of wood is at the low end of this scale and aromatic fuels are at the high end.
- For the large fires of most consequence, there is little expected change in the nature of the smoke as one moves further from the fire room.
  - Changes in respirability resulting from changes in aerosol dimension are expected to be modest. An exception may be the mitigation of the high toxicity of PFP fumes through aggregation of ultrafine particles.
  - The total smoke wall loss from fires in buildings is predicted to be a small fraction of the total smoke generated.
  - Losses of gas phase toxicants from the breathable atmosphere are also expected to be relatively modest.
- Surface adsorption of gases on the smoke aerosol surface is likely to be small compared to the amount of the gas needed for a toxic effect.
- It is possible for toxicologically significant quantities of polar gases, such as halogen acids, to dissolve in water droplets.

### Research Needs

The quality of fire hazard and risk assessment with regard to toxicants in smoke would be improved by:

- Measurement of mass median aerodynamic diameter of soot agglomerates avoiding possible agglomerate structural changes with impactors.

- Quantitative information on the adsorption of irritant gases on fire generated soot aerosol;
- Quantitative information on the losses of toxicants to walls for a range of realistic fires.
- Development of model for predicting smoke aerosol and vapor loss to the walls for a fire in an enclosure.
- Information on the size distribution of water droplets at fires, the conditions under which they are formed, and the amount of gases adsorbed on the droplets.
- Understanding the role of nanoparticles regarding the toxic effect of PCP fumes.

## References

- [1] D.A. Purser, "Toxicity Assessment of Combustion Products," in *The SFPE Handbook of Fire Protection Engineering*, P.J. DiNenno et al. Eds., 3rd ed., Quincy, MA: National Fire Protection Association, 2002, sec. 2, chap. 6.
- [2] I.M. Kennedy, "Models of Soot Formation and Oxidation," *Progress in Energy and Combustion Science*, vol. 23, 1997, pp. 95–132.
- [3] S. Leonard, G.W. Mulholland, R. Puri, and R.J. Santoro, "Generation of CO and Smoke During Underventilated Combustion," *Comb. and Flame*, vol. 98, 1994, pp. 20–34.
- [4] G.W. Mulholland, V. Henzel, and V. Babrauskas, "The Effect of Scale on Smoke Emission," in *International Association for Fire Safety Science: Fire Safety Science, Proceedings of the Second International Symposium*, Tokyo, Japan, June 13–17, 1988, New York: Hemisphere Publishing Corp., 1989, pp. 347–357.
- [5] A. Tewarson, "Generation of Heat and Chemical Compounds in Fires," in *The SFPE Handbook of Fire Protection Engineering*, P.J. DiNenno et al. Eds., 3rd ed., Quincy, MA: National Fire Protection Association, 2002, sec. 3, chap. 4.
- [6] D.D. Evans, W.D. Walton, H.R. Baum, K.A. Notarianni, J.R. Lawson, H.C. Tang, K.R. Keydel, R.G. Rehm, D. Madrzykowski, R.H. Zile, H. Koseki, and E.J. Tennyson, "In-Situ Burning of Oil Spills: Mesoscale Experiments," in *Proceedings of the Fifteenth Arctic and Marine Oil Spill Program Technical Seminar*, Edmonton, Alberta, June 10–12, 1992, Ministry of Supply and Services Canada Cat. No. En 40-11/5-1992, 1992, pp. 593–657.
- [7] A. Tewarson, F.H. Jiang, and T. Morikawa, "Ventilation-Controlled Combustion of Polymers," *Comb. and Flame*, vol. 95, 1993, pp. 151–169.
- [8] R.L. Dod, N.J. Brown, F.W. Mowrer, T. Novakov, and R.B. Williamson, "Smoke Emission Factors from Medium-Scale Fires: Part 2," *Aerosol Science and Technology*, vol. 10, no. 1, 1989, pp. 20–27.
- [9] D.A. Purser, "Recent Developments in Understanding the Toxicity of PTFE Thermal Decomposition Products," *Fire and Materials*, vol. 16, 1992, pp. 67–75.
- [10] Ü.Ö. Köylü and G.M. Faeth, "Optical Properties of Overfire Soot in Buoyant Turbulent Diffusion Flames at Long Residence Times," *Journal of Heat Transfer*, vol. 116, 1994, pp. 152–159.
- [11] R.J. Samson, G.W. Mulholland, and J.W. Gentry, "Structural Analysis of Soot Agglomerates," *Langmuir*, vol. 3, 1987, pp. 272–281.
- [12] C.M. Sorensen, J. Cai, and N. Lu, "Light-Scattering Measurements of Monomer Size, Monomers per Aggregate, and Fractal Dimension for Soot Aggregates in Flames," *Applied Optics*, vol. 31, 1992, pp. 6547–6557.
- [13] C.M. Sorensen, "Light Scattering by Fractal Aggregates: A Review," *Aerosol Science and Technology*, vol. 35, 2001, pp. 648–687.
- [14] R.D. Mountain and G.W. Mulholland, "Light Scattering from Simulated Smoke Agglomerates," *Langmuir*, vol. 4, 1988, pp. 1321–1326.

- [15] P. Meakin, "Diffusion Limited Aggregation in Three Dimensions: Results from a New Cluster-Cluster Aggregation Model," *Journal of Colloid and Interface Science*, vol. 102, 1984, pp. 491–512.
- [16] C.M. Sorensen and G.C. Roberts, "The Prefactor of Fractal Aggregates," *Journal of Colloid and Interface Science*, vol. 186, 1997, pp. 447–452.
- [17] W.C. Hinds, *Aerosol Technology; Properties, Behavior, and Measurement of Airborne Particles*, New York: John Wiley and Sons, 1982.
- [18] P.C. Reist, *Introduction to Aerosol Science*, New York: Macmillan Publishing Co., 1984.
- [19] O.G. Raabe, "Particle Size Analysis Utilizing Grouped Data and the Log-Normal Distribution," *Aerosol Science*, vol. 2, 1971, pp. 289–303.
- [20] G.W. Mulholland, "Smoke Production and Properties," in *The SFPE Handbook of Fire Protection Engineering*, P.J. DiNunno et al. Eds., 2nd ed., Quincy, MA: National Fire Protection Association, 1995, sec. 2, chap. 15.
- [21] T.G. Cleary, "Measurements of the Size Distribution and Aerodynamic Properties of Soot," Ph.D. thesis, College Park, MD: University of Maryland, 1989.
- [22] L. Waldmann and K.H. Schmitt, "Thermophoresis and Diffusiophoresis of Aerosols," in *Aerosol Science*, C.N. Davies Ed., New York: Academic Press, 1966, chap. VI.
- [23] M.D. Allen and O.G. Raabe, "Slip Correction Measurements of Spherical Solid Aerosol Particles in an Improved Millikan Apparatus," *Aerosol Science and Technology*, vol. 4, no. 3, 1985, pp. 269–286.
- [24] A. Gomez and D.E. Rosner, "Thermophoretic Effects on Particles in Counterflow Laminar Diffusion Flames," *Combustion Science and Technology*, vol. 89, 1993, pp. 335–362.
- [25] G.M. Wang and C.M. Sorensen, "Diffusion Mobility of Fractal Aggregates over the Entire Knudsen Number Range," *Physical Review E*, vol. 60, 1999, pp. 3036–3044.
- [26] S.N. Rogak, R.C. Flagan, and H.V. Nguyen, "The Mobility and Structure of Aerosol Agglomerates," *Aerosol Science and Technology*, vol. 18, no. 1, 1993, pp. 25–47.
- [27] A. Schmidt-Ott, "In Situ Measurement of the Fractal Dimensionality of Ultrafine Aerosol Particles," *Applied Physics Letters*, vol. 52, no. 12, 1988, pp. 954–956.
- [28] R.A. Dobbins, G.W. Mulholland and N.P. Bryner, "Comparison of a Fractal Smoke Optics Model with Light Extinction Measurements," *Atmospheric Environment*, vol. 28, no. 5, 1994, pp. 889–897.
- [29] G.K. Batchelor and C. Shen, "Thermophoretic Deposition of Particles in Gas Flowing Over Cold Surfaces," *Journal of Colloid and Interface Science*, vol. 107, no. 1, 1985, pp. 21–37.
- [30] D.E. Rosner, D.W. Mackowski, M. Tassopoulos, J. Castillo, and P. Garcia-Ybarra, "Effects of Heat Transfer on the Dynamics and Transport of Small Particles Suspended in Gases," *Industrial and Engineering Chemistry Research*, vol. 31, no. 3, 1992, pp. 760–769.
- [31] Personal communication from Howard R. Baum, 2000.
- [32] S.K. Friedlander, *Smoke, Dust, and Haze*, New York: John Wiley and Sons, 1997.
- [33] G.W. Mulholland, T.G. Lee, and H.R. Baum, "The Coagulation of Aerosols with Broad Initial Size Distribution," *Journal of Colloid and Interface Science*, vol. 62, no. 3, 1977, pp. 406–420.
- [34] D.D. Evans, H.R. Baum, G.W. Mulholland, N.P. Bryner, and G.P. Forney, "Smoke Plumes from Crude Oil Burns," in *Proceedings of the Twelfth Arctic and Marine Oil Spill Program Technical Seminar*, Calgary, Alberta, June 7–9, 1989, Ministry of Supply and Services Canada Cat. no. En 40-11/5-1989, 1989, pp. 1–22.
- [35] S.J. Gregg and K.S.W. Sing, *Adsorption, Surface Area and Porosity*, 2nd ed., New York: Academic Press, 1982.
- [36] G.F. Cerefolini and W. Rudziński, "Theoretical Principles of Single- and Mixed-Gas Adsorption Equilibria on Heterogeneous Solid Surfaces," in *Equilibria and Dynamics of Gas Adsorption on Heterogeneous Solid Surfaces*, W. Rudziński et al., Eds., Amsterdam, The Netherlands: Elsevier Science B.V., 1997, pp. 1–104.

- [37] W. Rudziński, W.A. Steele, and G. Zgrablich (eds.), *Equilibria and Dynamics of Gas Adsorption on Heterogeneous Solid Surfaces*, Amsterdam, The Netherlands: Elsevier Science B.V., 1997.
- [38] A.R. Chughtai, G.R. Williams, M.M.O. Atteya, N.J. Miller, and D.M. Smith, "Carbonaceous Particle Hydration," *Atmospheric Environment*, vol. 33, no. 17, 1999, pp. 2679–2687.
- [39] P.N. Cheremisinoff and A.C. Morresi, "Carbon Adsorption Applications," in *Carbon Adsorption Handbook*, P.N. Cheremisinoff and F. Ellerbusch, Eds., Ann Arbor, MI: Ann Arbor Science Publ., Inc., 1978, pp. 1–53.
- [40] J.T. Cookson, Jr., "Adsorption Mechanisms: The Chemistry of Organic Adsorption on Activated Carbon," in *Carbon Adsorption Handbook*, P.N. Cheremisinoff and F. Ellerbusch, Eds., Ann Arbor, MI: Ann Arbor Science Publ., Inc., 1978, pp. 241–279.
- [41] D.J. Lary, D.E. Shallcross, and R. Toumi, "Carbonaceous Aerosols and Their Potential Role in Atmospheric Chemistry," *Journal of Geophysical Research—Atmospheres*, vol. 104, no. D13, 1999, pp. 15,929–15,940.
- [42] K.-U. Goss and S.J. Eisenreich, "Sorption of Volatile Organic Compounds to Particles from a Combustion Source at Different Temperatures and Relative Humidities," *Atmospheric Environment*, vol. 31, no. 17, 1997, pp. 2827–2834.
- [43] K. Kaneko, "Heterogeneous Surface Structures of Adsorbents," in *Equilibria and Dynamics of Gas Adsorption on Heterogeneous Solid Surfaces*, W. Rudziński et al., Eds., Amsterdam, The Netherlands: Elsevier Science B.V., 1997, pp. 679–714.
- [44] M. Kruk and M. Jaroniec, "Gas Adsorption Characterization of Ordered Organic-Inorganic Nanocomposite Materials," *Chemistry of Materials*, vol. 13, 2001, pp. 3169–3183.
- [45] M. Jaroniec and J. Choma, "Characterization of Geometrical and Energetic Heterogeneities of Active Carbons by Using Sorption Measurements," in *Equilibria and Dynamics of Gas Adsorption on Heterogeneous Solid Surfaces*, W. Rudziński et al., Eds., Amsterdam, The Netherlands: Elsevier Science B.V., 1997, pp. 715–744.
- [46] A.R. Chughtai, M.M.O. Atteya, J. Kim, B.K. Konowalchuk, and D.M. Smith, "Adsorption and Adsorbate Interaction at Soot Particle Surfaces," *Carbon*, vol. 36, no. 11, 1998, pp. 1573–1589.
- [47] E.F. Mikhailov, S.S. Vlasenko, L. Krämer, and R. Niessner, "Interaction of Soot Aerosol Particles with Water Droplets: Influence of Surface Hydrophilicity," *Aerosol Science*, vol. 32, 2001, pp. 697–711.
- [48] F.M. Galloway and M.M. Hirschler, "A Model for the Spontaneous Removal of Airborne Hydrogen Chloride by Common Surfaces," *Fire Safety Journal*, vol. 14, no. 4, 1989, pp. 251–268.
- [49] L.Y. Cooper, "Convective Heat Transfer to Ceilings Above Enclosure Fires," in *19th Symposium (International) on Combustion*, Haifa, Israel, August 8–13, 1982, Philadelphia, PA: Combustion Institute, 1982, pp. 933–939.
- [50] W.W. Jones, "A Model for the Transport of Fire, Smoke and Toxic Gases (FAST)," NBSIR 84-2934, National Bureau of Standards, 1984.
- [51] F.M. Galloway and M.M. Hirschler, "The Use of a Model for Hydrogen Chloride Transport and Decay to Predict Airborne Hydrogen Chloride Concentrations in a Full-Scale Room—Corridor Scenario," *Fire Safety Journal*, vol. 19, no. 1, 1992, pp. 73–101.
- [52] F.M. Galloway and M.M. Hirschler, "Transport and Decay of Hydrogen Chloride: Use of a Model to Predict Hydrogen Chloride Concentrations in Fires Involving a Room—Corridor—Room Arrangement," *Fire Safety Journal*, vol. 16, no. 1, 1990, pp. 33–52.
- [53] K.B. McGrattan, H.R. Baum, R.G. Rehm, A. Hamins, and G.P. Forney, "Fire Dynamics Simulator—Technical Reference Guide," NISTIR 6467, Gaithersburg, MD: National Institute of Standards and Technology, 2000.
- [54] J.P. Stone, R.N. Hazlett, J.E. Johnson, and H.W. Carhart, "The Transport of Hydrogen Chloride by Soot from Burning Polyvinyl Chloride," *Journal of Fire and Flammability*, vol. 4, no. 1, 1973, pp. 42–51.

- [55] J.P. Stone, "Transport of Hydrogen Chloride by Water Aerosol in Simulated Fires," *JFF/Combustion Toxicology*, vol. 2, no. 2, 1975, pp. 127–138.
- [56] J.P. Stone and F.W. Williams, "Transport of Hydrogen Cyanide by Water Aerosol in a Simulated Fire Atmosphere," *Journal of Combustion Toxicology*, vol. 4, no. 2, 1977, pp. 231–235.
- [57] K. Donaldson, X.Y. Li, and W. MacNee, "Ultrafine (Nanometre) Particle Mediated Lung Injury," *Journal of Aerosol Science*, vol. 29, nos. 5/6, 1998, pp. 553–560.
- [58] C.A. Pope III, "Epidemiology of Fine Particulate Air Pollution and Human Health: Biologic Mechanisms and Who's at Risk?" *Environmental Health Perspectives*, vol. 108, Suppl., 2000, pp. 713–723.
- [59] T.R. Sosnowski, L. Gradon, and A. Podgórski, "Influence of Insoluble Aerosol Deposits on the Surface Activity of the Pulmonary Surfactant: A Possible Mechanism of Alveolar Clearance Retardation?" *Aerosol Science and Technology*, vol. 32, no. 1, 2000, pp. 52–60.
- [60] A. Churg, B. Gilks, and J. Dai, "Induction of Fibrogenic Mediators by Fine and Ultrafine Titanium Dioxide in Rat Tracheal Explants," *American Journal of Physiology—Lung Cellular and Molecular Physiology*, vol. 277, no. 5, 1999, pp. L975–L982.
- [61] B.C. Levin, "The National Bureau of Standards Toxicity Test Method," *Fire Technology*, vol. 21, no. 2, 1985, pp. 134–145.
- [62] P.J. Fardell, "UK Studies of the Toxic Potency of PTFE in Fire," in *Proceedings of Interflam '90, 5th International Fire Conference*, Canterbury, England, September 3–6, 1990, London, England: Interscience Communications Ltd., 1990, pp. 257–271.
- [63] F.B. Clarke, H. van Kuijk, R. Valentine, G.T. Makovec, W.C. Seidel, B.B. Baker, Jr., D.J. Kasprzak, J.K. Bonesteel, M. Janssens, and C. Herpol, "The Toxicity of Smoke from Fires Involving Perfluoropolymers: Full-Scale Fire Studies," *Journal of Fire Sciences*, vol. 10, 1992, pp. 488–527.
- [64] F.B. Clarke, W.C. Seidel, K.V. Scherer, D. Cline, A. Olson, and J.K. Bonesteel, "Formation, Identity and Coagulation of Fluoropolymer-Derived Smoke Aerosols. The Relationship Between Aerosol Behavior and Observed Toxicity of Fluoropolymer Smoke," in *Proceedings of Interflam '90, 5th International Fire Conference*, Canterbury, England, September 3–6, 1990, London, England: Interscience Communications Ltd., 1990, pp. 297–304.
- [65] C.J. Johnston, J.N. Finkelstein, R. Gelein, R. Baggs, G. Oberdörster, "Characterization of the Early Pulmonary Inflammatory Response Associated with PTFE Fume Exposure," *Toxicology and Applied Pharmacology*, vol. 140, no. 1, 1996, pp. 154–163.
- [66] C.J. Johnston, J.N. Finkelstein, P. Mercer, N. Corson, R. Gelein, and G. Oberdörster, "Pulmonary Effects Induced by Ultrafine PTFE Particles," *Toxicology and Applied Pharmacology*, vol. 168, 2000, pp. 208–215.
- [67] T.G. Lee and G.W. Mulholland, "Physical Properties of Smokes Pertinent to Smoke Detector Technology," NBSIR 77-1312, Gaithersburg, MD: National Bureau of Standards, 1977.
- [68] R.J. Samson, G.W. Mulholland, and J.W. Gentry, "Structural Analysis of Soot Agglomerates," *Langmuir*, vol. 3, no. 2, 1987, pp. 272–281.
- [69] R.C. Corlett and G.A. Cruz, "Smoke and Toxic Gas Production in Enclosed Fires," *JFF/Combustion Toxicology*, vol. 2, no. 1, 1975, pp. 8–33.
- [70] D. Evans, G. Mulholland, D. Gross, H. Baum, and K. Saito, "Environmental Effects of Oil Spill Combustion," NISTIR 88-3822, Gaithersburg, MD: National Bureau of Standards, 1988; also in *Proceedings of the Tenth Arctic and Marine Oil Spill Program Technical Seminar*, Edmonton, Alberta, June 9–11, 1987, Ministry of Supply and Services Canada, Cat. no. En 40-11/5-1987E, 1987, pp. 91–130.
- [71] C.P. Bankston, R.A. Cassanova, E.A. Powell, and B.T. Zinn, "Review of Smoke Particulate Properties Data for Burning Natural and Synthetic Materials," NBS-GCR 78-147, Gaithersburg, MD: National Bureau of Standards, 1978.

- [72] R.L. Dod, F.W. Mowrer, L.A. Gundel, T. Novakov, and R.B. Williamson, "Size Fractionation of Black and Organic Particulate Carbon from Fires. Final Report," LBL-20654, Berkeley, CA: Lawrence Berkeley Laboratory, 1985.
- [73] E.M. Patterson, R.M. Duckworth, C.M. Wyman, E.A. Powell, and J.W. Gooch, "Measurements of the Optical Properties of the Smoke Emissions from Plastics, Hydrocarbons, and Other Urban Fuels for Nuclear Winter Studies," *Atmospheric Environment*, vol. 25A, no. 11, 1991, pp. 2539–2552.
- [74] C.J. Hilado, *Flammability Handbook for Electrical Insulation*, Westport, CN: Technomic Publishing Co., 1982.